JOURNAL OF Applied Polymer SCIENCE

# Optical Characterization and Differential Scanning Calorimetry Studies of Carboxymethyl Cellulose–Nickel Chloride Composite System

**Farid M. Abdel-Rahim,[1,2] K. H. Mahmoud,[3,4] K. A. Aly[1,2]**

[1]Physics Department, Faculty of Science & Arts (Khulais), King Abdul Aziz University, Jeddah, Saudi Arabia
[2]Physics Department, Faculty of Science Branch Assiut, Al Azhar University, Assuit, Egypt
[3]Physics Department, Faculty of Science, Taif University, Taif, Saudi Arabia
[4]Physics Department, Cairo University, Faculty of Science, Cairo, Egypt
Correspondence to: F. M. Abdel-Rahim (E-mail: farid.elkhateb@gmail.com, falkhateeb@kau.edu.sa)

**ABSTRACT:** Carboxymethyl cellulose (CMC) films doped with nickel chloride hexahydrate have been prepared by casting technique. The phase transitions and thermal stability of the prepared samples were investigated by differential scanning calorimetry and thermogravimetry. The optical absorption was recorded at room temperature in the wavelength range of 190–2500 nm. From the absorption edge studies, the values of the Urbach energy ($E_e$) were found to be 0.58 eV in case of the pure polymer; however, the Urbach energy values were found to be in the range of 0.64–1.0 eV under additional different percentages of nickel chloride. These energy values indicate that the model based on random fluctuations of the internal fields associated with structure disorder is preferable and transitions are made between band tails. Refractive index, complex dielectric constants have also been determined. Color properties of the prepared samples are discussed in the frame work of CIE $L^*u^*v^*$ color space. © 2012 Wiley Periodicals, Inc. J. Appl. Polym. Sci. 000: 000–000, 2012

**KEYWORDS:** polymers; differential scanning calorimetry (DSC); thermal properties; optical properties; dielectric properties and color centers

Received 28 January 2012; accepted 14 May 2012; published online 00 Month 2012
**DOI: 10.1002/app.38060**

## INTRODUCTION

Polymers combined with metal salts are useful for the development of the advanced high-energy electrochemical devices such as batteries, fuel cells, electrochemical display devices, and photo electrochemical cells.[1–5] Also, they have been successfully employed in areas such as removal of harmful trace metal ions, because of their highly selective adsorptivity for heavy metal ions. They have also been given much attention with respect to the recovery of rare metal ions of great value and production of colors which have different applications.[6,7]

In recent years, $Ni^{+2}$-doped optical materials have received much attention.[8–12] The initial and terminal states of the electronic transition are strongly coupled to the lattice phonon modes and the associated emission bandwidth becomes much broader than that of rare-earth ions such as $Er^{+3}$, $Nd^{+3}$, $Pr^{+3}$, and so on. Thus, the emission usually covers the wavelength range of 1100–1600 nm. Much of the present interest centers on the possibility of $Ni^{+2}$-doped materials as active media for broadband optical amplifiers and tunable near-infrared laser systems. Nickel behaves as coloring agent in various materials for different applications.[13]

CMC is one of the important cellulose derivatives and generally prepared through the reaction of alkali cellulose with monochloroacetate or its sodium salt in organic mediums. It is nontoxic water-soluble polymer possess many available qualities, such as filming, emulsification, suspension, water maintaining, bind, and inspissations. Therefore, it has been used for many applications such as medicine, food, textures, electrical elements, papermaking, printing, and dyeing.

Therefore, this study is devoted to prepare a composite system between $NiCl_2$ and CMC polymer and study the effect of $Ni^{2+}$ ion on thermal and optical properties of composites to probe their uses in the industrial applications.

## EXPERIMENTAL

### Materials

CMC with molecular weight approximately 250,000 was supplied by BDH Chemical Advantec Toyoroshi, Japan. Poole England and nickel chloride hexahydrate were supplied by BDH Chemical Advantec Toyoroshi, Japan.

**Table I.** Designation of X $NiCl_2$ − (100 − *X*) CMC Composite System

| *X* (wt %) | Polymer composition | Polymer number |
|---|---|---|
| 0 | CMC | C0 |
| 5 | 95 CMC—5 $NiCl_2$ | C5 |
| 10 | 90 CMC—10 $NiCl_2$ | C10 |
| 20 | 80 CMC—20 $NiCl_2$ | C20 |
| 40 | 60 CMC—40 $NiCl_2$ | C40 |

## Methods

**Preparation of Samples.** The solution method was used to obtain film samples. Weighed amounts of CMC were dissolved in a mixture of distilled water and ethanol (ratio, 4 : 1) using a magnetic stirrer at 50°C on water bath for 4 h. The appropriate weighed amounts of $NiCl_2$ were dissolved in distilled water at room temperature. Solutions of CMC were mixed with $NiCl_2{\cdot}6H_2O$ to give 5, 10, 20, and 40 wt % of Ni-doped CMC using magnetic stirrer at 60–80°C. The samples' designation is summarized in Table I. Films of suitable thickness (∼50 μm) were casted onto stainless steel Petri dishes, and then dried in an open air at room temperature (about 30°C) for about 6 days until solvent was completely evaporated.

**Thermal Analysis.** Thermal analysis was carried out using a computerized differential scanning calorimetry (DSC) and thermogravimetric analysis (TGA) Shimadzu-50, Kyoto, Japan. Measurements were carried out under nitrogen atmosphere (30 mL/min).

**Spectroscopic Analysis.** The absorption spectra of the samples were performed using Perkin-Elmer lambda 4$\beta$ spectrophotometer over the range of 190–2500 nm. The tristimulus transmittance values (*X, Y, Z*) were calculated using the transmittance data obtained in the visible range according to CIE $L^*u^*v^*$ system. Also, the CIE three-dimensional ($L^*$, $U^*$, $V^*$) color constants, whiteness (*W*), yellowness (*Y*), chroma ($C^*$), hue and color difference ($\Delta E$) were performed.

## RESULTS AND DISCUSSION

### Thermal Analysis

The thermal properties of composite system were determined by DSC to investigate the effect of $Ni^{+2}$ concentrations on the thermal transitions of CMC (C0 sample). Figure 1 shows that the pure CMC and those doped with $Ni^{+2}$ give a broad and a relatively large glass transition temperature ($T_g$). It was observed that $T_g$ decreases with the $Ni^{+2}$ content increasing which leads to the decrease of polymer rigidity. Furthermore, there are sharp three exothermic peaks at 547, 595, and 643 K, respectively, for pure polymer. These exothermic peaks correspond to degradation.[14] Although the $Ni^{+2}$ content increases, the endothermic peaks were appeared at 504 and 649 K for C40 sample. These two endothermic peaks can be attributed to thermal decomposition of the doped polymer. In case of pure polymer, the initial weight loss of ∼16.0% up to 544 K is owing to the removal of moisture present in the polymer. An extremely large weight loss of ∼20% up to 639 K suggests that the CMC still contains some volatile material as summarized in Table II.

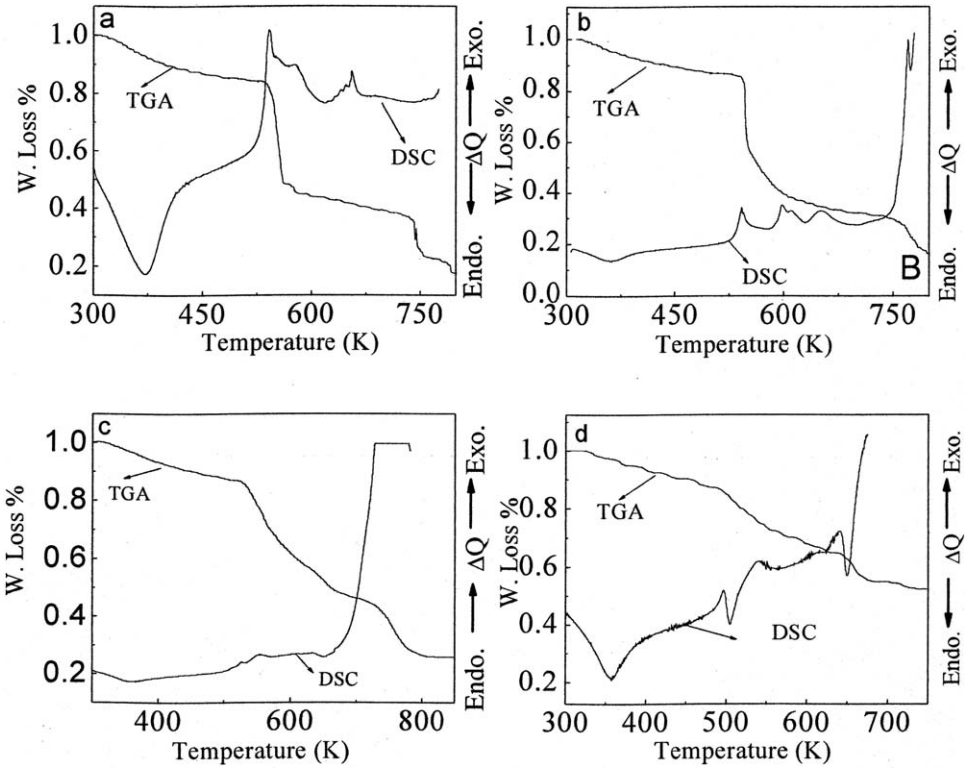


**Figure 1.** The DSC and TGA thermograms results for *X* $NiCl_2$ − (100 − *X*) CMC composite system.

**Table II.** DSC and TGA results for *X* $NiCl_2$ − (100 − X) CMC Composite System[a]

| | DSC | | TGA | |
|---|---|---|---|---|
| Polymer number | Peak temp. (K) | Comment | Temp. range (K) | Loss (wt %) |
| C0 | | | | |
| | 377 | Endo | 303-543.5 | 16.49 |
| | 547.88 | Exo | 543.5-638.8 | 38.28 |
| | 595 | Exo | 638.8-675.8 | 3.95 |
| | 643.53 | Exo | 675.8-750 | 2.43 |
| C5 | | | | |
| | 372.03 | Endo | 303-534 | 16.8 |
| | 541.71 | Exo | 534-555 | 18.71 |
| | 555.35 | Exo | 555-576 | 3.61 |
| | 576.17 | Exo | 576-694 | 8.32 |
| | 655.6 | Exo | 694-750 | 13.6 |
| C10 | | | | |
| | 361 | Endo | 303-542 | 17.2 |
| | 542.59 | Exo | 542-553 | 28.47 |
| | 598 | Exo | 553-608 | 18.4 |
| | 610 | Exo | 608-750 | 9.0 |
| | 651.93 | Exo | | |
| C20 | | | | |
| | 360 | Endo | 300-528 | 14 |
| | 526 | Exo | 528-673 | 38 |
| | 553 | Exo | 673-750 | 11 |
| | 611 | Exo | | |
| | 633 | Exo | | |
| CMC 40 | | | | |
| | 357.96 | Endo | 303-488 | 13.6 |
| | 497 | Exo | 488-557 | 14.6 |
| | 504.82 | Endo | 557-644.7 | 9.25 |
| | 538.56 | Exo | 644.7-750 | 11.93 |
| | 641.24 | Exo | | |
| | 649.12 | Endo | | |

[a]Endo, endothermic peak; Exo, exothermic peak.

## Optical Properties

**Optical Absorption Analysis.** The measurements of the optical absorption and the absorption edge are important, especially in connection with the theory of electronic structure of amorphous materials. The spectrum of the doped samples (Figure 2) shows an ultraviolet cutoff region whose width increases up to 235 nm under addition of $Ni^{+2}$ ions. The cutoff region comprises two peaks at 195 and 205 nm and a visible band at approximately 400 nm. The peaks appeared at 195 and 205 are assigned to $n$-$\pi^*$ electronic transition (R-band) of chromophoric groups in CMC.[15] It is well known that $Ni^{+2}$ in the octahedral symmetrical field possesses three spin-allowed transitions and two spin-forbidden transitions as well.[16] Accordingly, it is reasonable to assign the absorption band observed at 400 nm to the spin-allowed transition $^3A_{2g}(^3F) \rightarrow {}^3T_{1g}(^3p)$. In addition, this band position seems to indicate the presence of $Ni^{+2}$ in the polymer matrix mostly in octahedral coordination and this assumption is supported by considering the large ligand field stabilization energy of $Ni^{+2}$ in octahedral symmetry compared with that in tetrahedral symmetry[17] (1.2 Δ for octahedral and 0.36 Δ for tetrahedral). $Ni^{+2}$ would generally be expected to occur preferably in octahedral symmetry.

Generally, the change in absorption spectrum of pure polymer (C0) under addition of $NiCl_2$ is an indication of chelate formation of $Ni^{2+}$ co-ordinated with the hydroxyl and carboxymethyl groups of CMC.[18]

**Optical Parameters.** The absorption coefficient, $\alpha(v)$ and near the edge of each curve was calculated, using the following equation[19]

$$\alpha(v) = \frac{-1}{d}\ln\left[\frac{(1-R)^2}{2TR^2} + \sqrt{\frac{(1-R)^4}{4T^2R^4} + \frac{1}{R^2}}\right] \quad (1)$$

where $d$ is the thickness of the film sample, $R$ is the reflectance, and $T$ is the transmittance of sample for incident photon. The absorption edge is observed in the UV region (Figure 2), depending on the value of the absorption coefficient ($\alpha$) for many amorphous materials. This region is usually known as Urbach tail[20] which is considered with $\alpha < 10^4$ $cm^{-1}$ and depends exponentially on the photon energy ($hv$) as showing in eq. (2):

$$\alpha(v) = ce^{\frac{hv}{E_e}} \quad (2)$$

The width of the band tails (Urbach energy $E_e$) associated with valence band and conduction bands was believed to be originated from the same physical origin. This origin is attributed to phonon-assisted indirect electronic transitions between localized states, where the density of these states is exponentially dependent on energy.[21] The Urbach energy arises from the random potential fluctuations in the material into the band gap.[22] The values of Urbach energy ($E_e$) were calculated by determining the reciprocal of the slopes of the linear regions of the curves as shown in Figure 3 and summarized in Table III.

It is noted that the pure polymer sample has the smallest Urbach energy ($E_e = 0.58$ eV) and sample 20 and 40 wt % Nickel chloride-doped CMC has the largest one ($E_e = 1$ eV). This can be explained on the basis that Urbach energy is generally used to characterize the degree of disorder in amorphous and crystalline solids. Materials with larger values of $E_e$ would have a great tendency to convert weak bonds into defects. Therefore, the value of Urbach energy is considered as a measure of defects' concentration.

**Complex Dielectric Constant and Refractive Index Dispersion.** The real ($\varepsilon'$) and imaginary ($\varepsilon''$) parts of complex dielectric constant can be calculated from the following equations:[23]

$$\varepsilon'(\lambda) = n^2(\lambda) - k^2(\lambda) \quad (3)$$

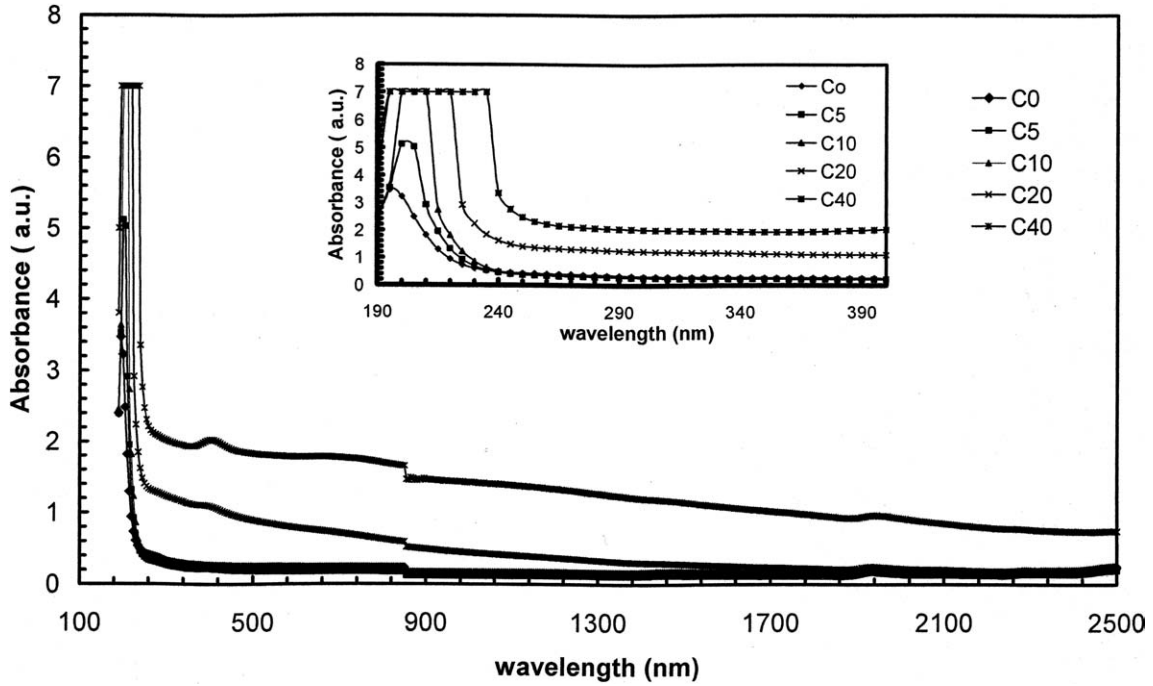


**Figure 2.** Absorption spectrum of $X$ $NiCl_2$ − (100 − $X$) CMC composite system.

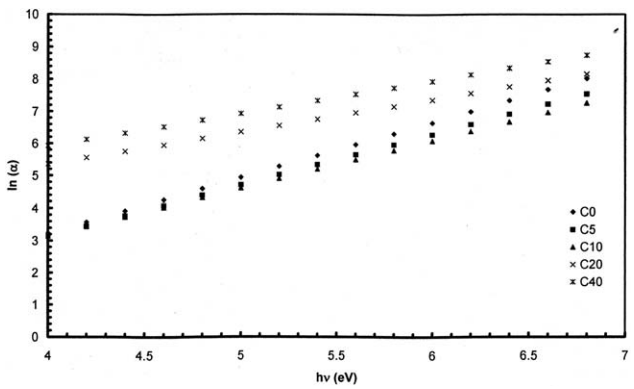


**Figure 3.** Urbach plots of $X$ $NiCl_2$ − (100 − $X$) CMC composite system.

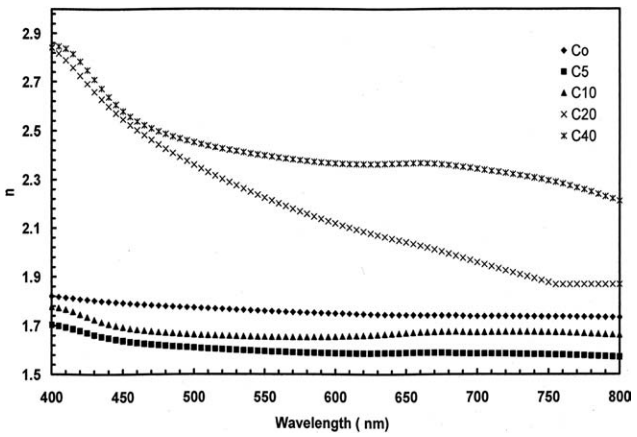


**Figure 4.** Dispersion of refractive index with wavelength for $X$ $NiCl_2$ − (100 − $X$) CMC composite system.

$$\varepsilon''(\lambda) = 2n(\lambda)\,k(\lambda) \tag{4}$$

where $n$ is the refractive index and $k$ is the extinction coefficient. The dispersion of refractive index is shown in Figure 4. It is seen that as wavelength increases the refractive index decreases until reaches a constant value $n_o$ (Table III). It is observed that as $Ni^{+2}$ concentration increases, the refractive index values increase but still less than its value for pure polymer in case of C5 and C10 samples and higher for other samples and this may be attributed to the variation of density and absorbance of samples under investigation. $\varepsilon'$ and $\varepsilon''$ are calculated for composite system at different incident photon energies and shown in Figure 5. We note that as $N^{+2}$ concentration increases $\varepsilon'$ and $\varepsilon''$ increase and this is owing to the increasing number of ionizable charges and dipoles for samples under investigation.[24]

**Color Measurements.** Figure 6 shows the variation of the tristimulus transmittance ($Y_t$) with wavelength in the range of 380–760 nm for composite samples (C0–C40). It is noticed that the behavior of $Y_t$ for all samples is similar as they have the same

**Table III.** Values of Energy Tail ($E_e$) and Refractive Index ($n_o$) for $NiCl_2$ − (100 − $X$) CMC Composite System

| Polymer number | $E_e$ (eV) | $n_o$ |
|---|---|---|
| C0 | 0.58 | 1.73 |
| C5 | 0.64 | 1.57 |
| C10 | 0.68 | 1.66 |
| C20 | 1.00 | 1.86 |
| C40 | 0.99 | 2.2 |

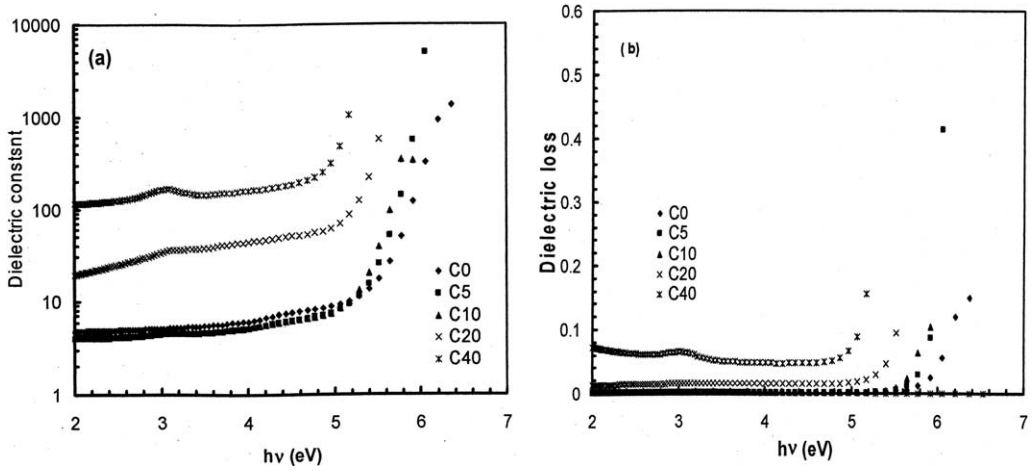


**Figure 5.** Variation of dielectric constant and loss with energy for of $X$ $NiCl_2$ − (100− $X$) CMC composite system.

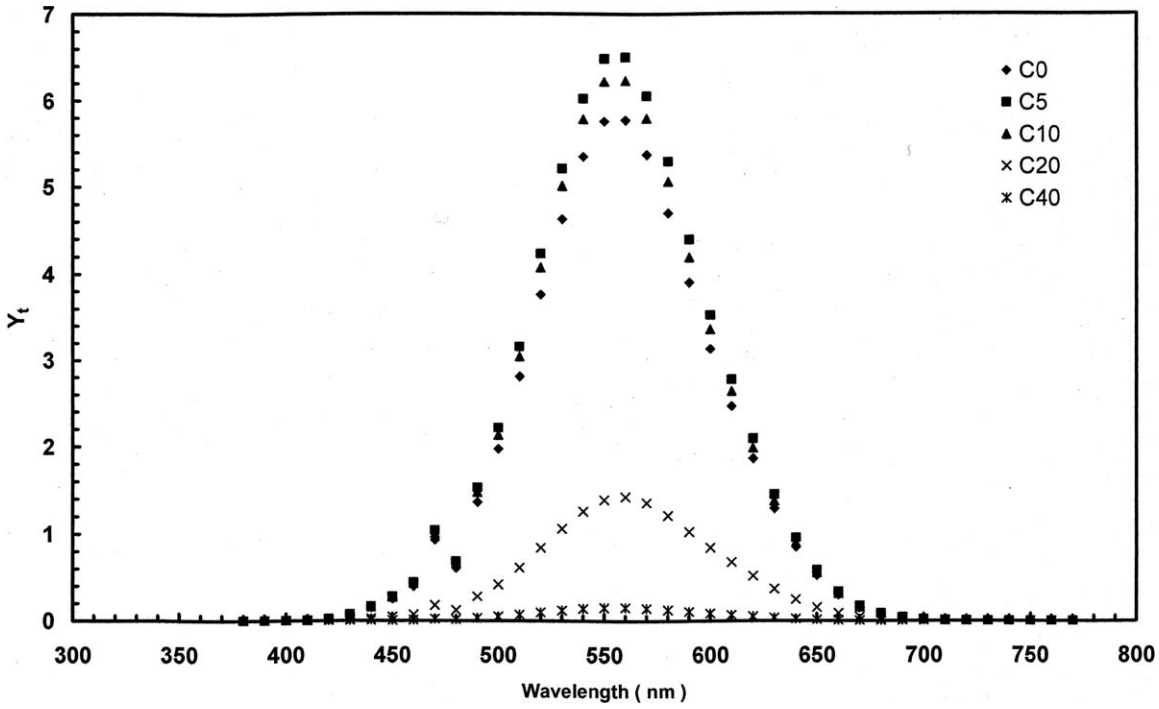


**Figure 6.** Tristimulus transmittance of $X$ $NiCl_2$ − (100 − $X$) CMC composite system.

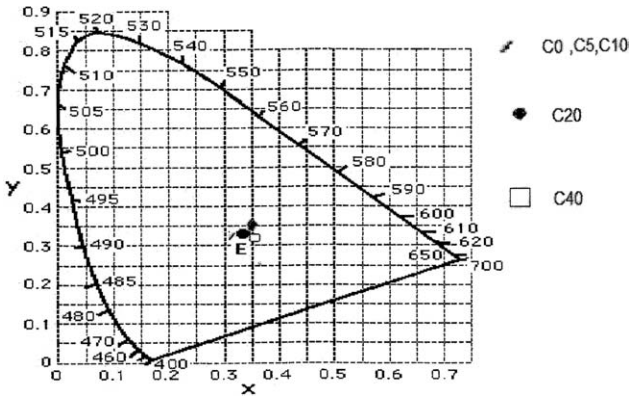


**Figure 7.** Chromaticity diagram of $X$ $NiCl_2$ − (100 − $X$) CMC composite system.

peak position at about 560 nm and a small peak at 470 nm. Also, it is observed that $Y_t$(max) changes irregularly with composition. The smallest and the highest $Y_t$(max) values were observed for the samples C40 and C5, respectively, and this was attributed to the transmission values.

Figure 7 shows the position of all samples on the chromaticity diagram and their distance to the white point. We see that all samples lie around white point ($E$). The locations of the samples are distinct from each other, and a clear color gradient is observed.

Table IV summarizes the color parameters $L^*$, $U^*$, $V^*$, $h_{ue}$, $W$, $Y_e^{25}$ and color difference data, $\Delta L^*$, $\Delta U^*$, $\Delta V^*$, $\Delta C^*$, $\Delta E$ between all samples and sample C0. We note that the color

**Table IV.** Color Parameters of $X$ $NiCl_2$ − (100 − $X$) CMC Composite System

| Polymer number | $L^*$ | $U^*$ | $V^*$ | $C^*$ | $\Delta L^*$ | $\Delta U^*$ | $\Delta V^*$ | $\Delta C^*$ | $\Delta E$ | $h_{ue}$ | $W$ | $Y_e$ |
|---|---|---|---|---|---|---|---|---|---|---|---|---|
| C0 | 81.07 | 0.73 | 1.84 | 1.98 | – | – | – | – | – | 68.33 | −700.91 | 0.26 |
| C5 | 84.97 | 0.64 | 3.26 | 3.33 | 3.90 | −0.09 | 1.42 | 1.42 | 4.15 | 78.86 | −78.88 | 0.04 |
| C10 | 83.51 | −0.24 | 2.53 | 2.54 | 2.44 | −0.75 | 0.69 | 1.02 | 2.64 | 95.50 | −755.22 | 0.03 |
| C20 | 44.75 | 7.68 | 14.43 | 16.35 | −36.32 | 6.95 | 12.95 | 14.69 | 39.18 | 61.96 | −172.03 | 0.37 |
| C40 | 12.86 | 0.73 | 3.27 | 3.35 | −68.21 | 0.00 | 1.43 | 1.43 | 68.22 | 77.41 | −18.43 | 0.24 |

parameters change irregularly with composition. The color difference data indicate that the sample C5 is lighter than the other samples. The sample C20 is redder, bluer, and more saturated than other samples; in addition, it has high $\Delta E$ value. The sample C40 is darker than other samples, has lowest redness and highest $\Delta E$ value.

## CONCLUSIONS

Polymer composite system based on CMC–$NiCl_2$ was prepared using a solvent casting technique. Thermal analysis techniques were performed to find out the different phase transitions and the thermal decomposition behavior of samples under study. DSC thermograms revealed that position of $T_g$ was shifted to lower temperatures as $NiCl_2$ content is increased. Optical measurements indicate the presence of $n$-$\pi^*$ electronic transitions which were interpreted in terms of Urbach transition mechanism. The change in absorption spectra is found to be limited to the position or intensity of the characteristic absorption bands. This effect is related to the role of divalent cation in the polymer structure and the ability of partly sharing as network forming groups. Experimental data indicate that the octahedral state of $Ni^{2+}$ slightly increases with the increase of the nickel content and this is correlated with the bond strength between the divalent cation and the polymer matrix and the extent of polarizability. The change of absorption spectra for the prepared samples enables us to use them as UV filters or shields. The color measurements show that there is an observable color gradient between CMC and other composite samples. Owing to the compositional dependence on optical measurements, these composites may be suitable for optical data storage.

## ACKNOWLEDGMENTS

This project was funded by the Deanship of Scientific Research (DSR), King Abdulaziz University, Jeddah, under grant no. (77/857/1431). The authors, therefore, acknowledge with thanks DSR technical and Financial support.

## REFERENCES

1. Abdelrazek, E. M.; Elashmawi, I. S.; El-Khodary, A.; Yassin, A. *Curr. Appl. Phys.* **2010,** *10*, 607.
2. Mahmoud, K. H.; El-Bahay, Z. M.; Hanafy, A. I. *J. Phys. Chem. Solids* **2011,** *72* 1057.
3. Ragab, H. M. *Phys. B* **2011,** *406*, 375.
4. Buerkle, A.; Sarabandi, K. *IEEE Trans. Antennas Propag.* **2005,** *53*, 3436.
5. El-Bahay, Z. M.; Mahmoud, K. H. *Spectrochem. Acta A* **2012,** *92*, 105.
6. Sugasaka, K.; Katoh, S.; Takai, N.; Takahashi, H.; Umezawa, Y. *Sep. Sci. Tech.* **1981,** *16*, 971.
7. Sakuragi, M.; Ichimura, K.; Fugishige, S.; Kateh, M. *Bull. Res. Inst. Polym. Text.* **1981,** *130*, 43.
8. Suzuki, T.; Ohishi, Y. *Appl. Phys. Lett.* **2004,** *84*, 3804.
9. Suzuki, T.; Arai, Y.; Ohishi, Y. J. *Lumin.* **2008,** *128*, 603.
10. Suzuki, T.; Ohishi, Y.; Tani, T. *Mater. Sci. Eng. B* **2006,** *128*, 151.
11. Feng, G.; Zhou, S.; Bao, J.; Wang, X.; Xu, S.; Qiu, J. J. *Alloy Compd.* **2008,** *457*, 506.
12. Wu, B.; Jiang, N.; Zhou, S.; Chen, D.; Zhu, C.; Qiu, J. *Opt. Mater.* **2008,** *30*, 1900.
13. Weyl, W. A.; Colored Glasses; Reprinted by Dawson's of Pall Mall, London, **1959.**
14. El-Sayed, S.; Mahmoud, K. H.; Fatah, A. A.; Hassen, A. *Phys. B* **2011,** *406*, 4068.
15. Barrow, G. M. Introduction to Molecular Spectroscopy, McGraw-Hill: New York, **1962;** p 271.
16. El-Batal, F. H.; Fayad, A. M.; El-Rahman, S. A.; Moustaffa, F. A. *Indian J. Pure Appl. Phys.* **2006,** *44*, 367.
17. Bates, T. In Modern Aspects of the Vitreous State, Mackenzie, J. D., Ed.; Butterworth: London, **1962; Vol.** *2*, Chapter 5, p 195.
18. Hossny, W. M.; Abdel Hady, A. K.; El-Saied, H.; Basta, A. H. *Polym. Int.* **1995,** *37*, 93.
19. Valalova, R.; Tichy, L.; Vlcek, M.; Ticha, H. *Phys. Status Solidi A* **2000,** *181*, 199.
20. Urbach, F. *Phys. Rev.* **1953,** *92*, 1324.
21. Tauc, J.; Zanini, M. J. *Non-Cryst. Solids* **1977,** *53*, 349.
22. Venkataraman, B. H.; Varma, K. B. *R. Opt. Mater.* **2006,** *28*, 1423.
23. Al-Ghamdi, A. A. *Vacuum* **2006,** *80*, 400.
24. Mahmoud, K. H.; Abdel-Rahim, F. M.; Atef, K.; Saddeek, Y. B. *Curr. Appl. Phys.* **2011,** *11*, 55.
25. Macadam, D. L., Color Measurements: Theme and Variation, Springer Series in Optical Sciences; Springer-Verlag: Berlin, Heidelberg, New York, **1981.**